Activation of Dual T Cell Signaling Pathways by the Chemokine RANTES

Kevin B. Bacon,*† Brett A. Premack,*† Phyllis Gardner, Thomas J. Schall

The chemokine RANTES induced biphasic mobilization of Ca^{2+} in T cells. The initial peak, a transient increase in cytosolic Ca^{2+} mediated by a heterotrimeric guanine nucleotide–binding protein (G protein)–coupled pathway, was associated predominantly with chemotaxis. The second peak, Ca^{2+} release and sustained influx dependent on protein tyrosine kinases, was associated with a spectrum of cellular responses—Ca^{2+} channel opening, interleukin-2 receptor expression, cytokine release, and T cell proliferation—characteristic of T cell receptor activation. Other chemokines did not produce these responses. Thus, in addition to inducing chemotaxis, RANTES can act as an antigen-independent activator of T cells in vitro.

RANTES is a potent chemoattractant cytokine (chemokine) for monocytes and T cells of the memory phenotype (*1*). The molecular mechanisms by which RANTES and other chemokines induce migration, and whether they are responsible for other regulatory effects on T cells, have not been thoroughly investigated. The chemokine receptors identified to date by molecular cloning all share a seven–transmembrane domain (7TM) architecture and thus are thought to be coupled to G proteins (*1*). Studies with monocytes and granulocytes have suggested that chemokine receptors may be linked to pertussis toxin (PTX)–sensitive G proteins (*2*); however, although G proteins have been implicated (*3*), the signal-transducing molecules in T cells are less well defined. In contrast to signaling by chemokines, a great deal of research has focused on T cell activation through the T cell antigen receptor (TCR) (*4*). As with many growth factor receptors, TCR signaling is independent of G protein activation and unaffected by PTX (*5*), but is abolished by the protein tyrosine kinase (PTK) inhibitors genistein and herbimycin A (HA) (*6*). Similar experiments with a variety of receptors and cell types have led to the widely accepted premise that most surface receptors signal through either PTK or G protein–coupled pathways.

In a normal human T cell clone (*7*) loaded with the fluorescent Ca^{2+} indicator indo-1 (*8*), RANTES applied at 1 to 100 nM induced a transient increase in cytosolic free Ca^{2+} concentration ($[Ca^{2+}]_i$) that peaked at 20 to 30 s and returned to resting values within 5 min (Fig. 1A). At 1 μM, however, RANTES elicited a biphasic $[Ca^{2+}]_i$ profile, consisting of a small early transient and a secondary larger and prolonged increase (*9*). The increase in $[Ca^{2+}]_i$ induced by 1 μM RANTES was of similar amplitude to that induced by stimulation of the TCR complex with saturating doses of antibody to CD3 (anti-CD3) (5 μg/ml) or the mitogen phytohemagglutinin (PHA) (10 μg/ml). However, TCR agonists elicited only the later, sustained phase of the Ca^{2+} response (Fig. 1B). Other chemokines that attract T cells—monocyte chemotactic protein–1 (MCP-1), macrophage inflammatory protein–1α (MIP-1α), and interleukin-8 (IL-8)—induced only the initial, transient increase in Ca^{2+}. In the presence of EGTA as an extracellular Ca^{2+} chelator, RANTES still induced a biphasic release of Ca^{2+} from intracellular stores, but both peaks were transient and reduced in amplitude (Fig. 1C). By 5 min after RANTES stimulation, >90% of the sustained increase in $[Ca^{2+}]_i$ was attributable to Ca^{2+} entry from the extracellular medium.

To examine the nature of the RANTES-activated Ca^{2+}-permeation pathway, we used the whole-cell configuration of the patch-clamp technique (*10*). In T cells clamped at −60 mV, a sustained inward current developed after a short lag (peaking at ~2 min) in response to 1 μM RANTES (Fig. 1D). Such currents were absent from unstimulated control cells. The whole-cell currents induced by RANTES were small (range of 9 to 14 pA at −60 mV), highly selective for divalent over monovalent cat-

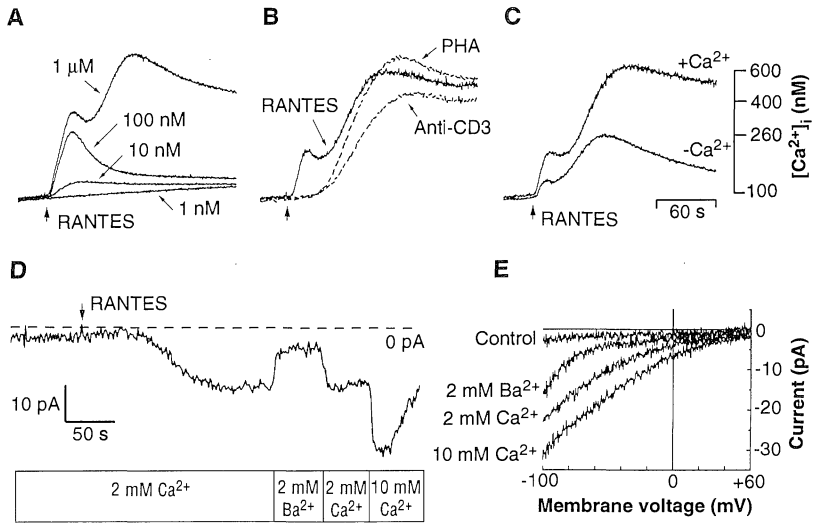

Fig. 1. RANTES-induced Ca^{2+} signaling in clonal human T cells. (**A**) Dose-dependent effect of RANTES at final concentrations of 1 nM to 1 μM on $[Ca^{2+}]_i$. Cells were suspended in a stirred cuvette and RANTES additions were made at the time indicated by the bold arrow (*8*). (**B**) Comparison of Ca^{2+} mobilization induced by RANTES (1 μM), anti-CD3 (5 μg/ml), and PHA (10 μg/ml). (**C**) The biphasic $[Ca^{2+}]_i$ profile observed with 1 μM RANTES results from two distinct phases of Ca^{2+} release followed by sustained Ca^{2+} influx. The increase in $[Ca^{2+}]_i$ observed in the presence of 2 mM extracellular Ca^{2+} (upper trace) was reduced by chelating extracellular Ca^{2+} with 3 mM EGTA (lower trace), revealing two phases of Ca^{2+} release from stores. The difference between the two traces reflects Ca^{2+} influx. (**D**) Biophysical properties of Ca^{2+} entry currents activated by RANTES in whole-cell patch-clamp experiments. At a holding potential of −60 mV, an inward Ca^{2+} current developed after a short delay following the addition of 1 μM RANTES. The current amplitude was reversibly reduced by substitution of external Ca^{2+} by Ba^{2+} (2 mM), indicating selectivity for Ca^{2+} over Ba^{2+}. Addition of 10 mM Ca^{2+} abruptly increased the current amplitude, further showing that the conductance is permeable to Ca^{2+}. (**E**) Whole-cell *I-V* curves recorded with voltage-ramp protocols. Four superimposed *I-V* curves comparing currents obtained before RANTES addition (in 2 mM Ca^{2+}) and after RANTES addition in solutions containing 2 mM Ba^{2+}, 2 mM Ca^{2+}, or 10 mM Ca^{2+} are shown. The voltage was ramped from −100 to +60 mV. Data shown in (D) and (E) were obtained from the same cell, which was representative of seven cells that responded to RANTES when studied with the whole-cell patch-clamp technique.

K. B. Bacon and T. J. Schall, Department of Immunology, DNAX Research Institute of Molecular and Cellular Biology, 901 California Avenue, Palo Alto, CA 94304, USA. B. A. Premack and P. Gardner, Department of Molecular Pharmacology, Stanford University School of Medicine, Stanford, CA 94305, USA.

*To whom correspondence should be addressed.
†These authors contributed equally to this work.

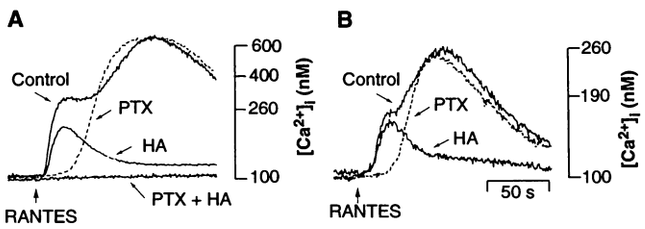

Fig. 2. Differential inhibition of the first and second phases of RANTES-induced Ca^{2+} mobilization by PTX and HA. (**A**) Incubation of clonal human T cells with PTX (100 ng/ml) for 18 hours selectively reduced the initial, transient phase, and incubation with HA (2 μM) for 18 hours inhibited the second, sustained phase, of Ca^{2+} mobilization. The combination of PTX with HA completely abolished all changes in $[Ca^{2+}]_i$ in response to 1 μM RANTES. Cells and recordings of $[Ca^{2+}]_i$ were analyzed as described for Fig. 1. (**B**) Dissection of two separable phases of Ca^{2+} release with PTX and HA in the absence of extracellular Ca^{2+}. PTX and HA each inhibited one component of the biphasic release of stored Ca^{2+}. Cells were incubated with inhibitors as in (A) and EGTA (3 mM) was added immediately before addition of RANTES.

ions (*11*), and mediated by Ca^{2+} to a greater extent than Ba^{2+} (Fig. 1D). Superimposed voltage-ramp, current-voltage (*I-V*) curves (−100 to +60 mV) (Fig. 1E) revealed inwardly rectifying currents that lack voltage-dependent gating and display a very positive (>+60 mV) reversal potential, as expected for a selective Ca^{2+} conductance. These properties are identical to those of the Ca^{2+} release–activated Ca^{2+} current (I_{crac}) (*12*) observed in the Jurkat T cell line after TCR stimulation, inositol trisphosphate release, or direct depletion of the Ca^{2+} stores (*13*). Thus, the Ca^{2+} release, sustained Ca^{2+} influx, and Ca^{2+} current properties suggest that RANTES mimics several of the earliest hallmarks of T cell activation.

The C-C chemokine receptor 1 (CKR-1), a 7TM receptor that binds RANTES (*14*), activates PTX-sensitive G proteins when expressed in human kidney cells (*15*). We therefore tested the effects of incubation with PTX (100 ng/ml) for 18 hours on cloned T cells. Whereas PTX completely and selectively inhibited the initial, transient phase of RANTES-induced Ca^{2+} mobilization (Fig. 2A), the magnitude and kinetics of the second, long-lasting peak of Ca^{2+} mobilization were unaffected. Because this second phase of the RANTES-induced Ca^{2+} response was similar to that seen after stimulation of T cells by anti-CD3 or PHA, a role for tyrosine phosphorylation in RANTES signaling was indicated. We therefore examined whether the PTX-insensitive Ca^{2+} entry pathway was affected by PTK inhibitors (*16*). HA, a selective inhibitor of Src family PTKs, inhibited in a potent and selective manner the second phase of the RANTES-induced Ca^{2+} response (50% inhibitory concentration, 0.2 μM), leaving the initial Ca^{2+} transient intact (Fig. 2A). PTX and HA appear to act by blocking the production of inositol trisphosphate rather than by inhibiting Ca^{2+} entry; in the absence of extracellular Ca^{2+}, each still selectively prevented one phase of Ca^{2+} release from stores (Fig. 2B). These results show that RANTES acts through two pharmacologically distinct signal transduction cascades, one linked to PTX-sensitive G proteins, and one to PTK activation. In addition, these pathways appear to be independent, because each remained unaltered when the other was fully inhibited.

To analyze further the role of PTKs, we performed immunoblot analysis of whole-cell lysates from quiescent cells (*17*) with antibodies to phosphotyrosine. Stimulation with RANTES increased phosphorylation of a large number of proteins between 30 and 200 kD (Fig. 3). The pattern and kinetics of phosphorylation induced by RANTES mimicked those induced by anti-CD3 or by PHA; the time course paralleled the plateau response of the second phase of Ca^{2+} mobilization. Phosphorylation induced by RANTES, PHA, or anti-CD3 was completely inhibited by HA (Fig. 3) (*9*).

The biological outputs of the G protein

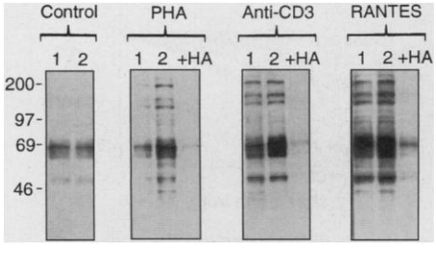

Fig. 3. Stimulation of tyrosine phosphorylation by RANTES. Untreated T cells or cells that had been pretreated with 2 μM HA were stimulated with 1 μM RANTES, anti-CD3 (5 μg/ml), or PHA (10 μg/ml), and cell lysates were resolved under reducing conditions by 10% SDS–polyacrylamide gel electrophoresis. Proteins were then transferred to Immobilon P membranes, which were incubated sequentially with antibodies to phosphotyrosine, horseradish peroxidase–conjugated secondary antibodies, and ECL reagent, and exposed to film. Lanes 1 and 2, 1 and 3 min after stimulation, respectively. All panels were loaded and exposed identically and are from a single representative blot. These results are typical of those obtained in five similar experiments. Molecular size standards are indicated in kilodaltons.

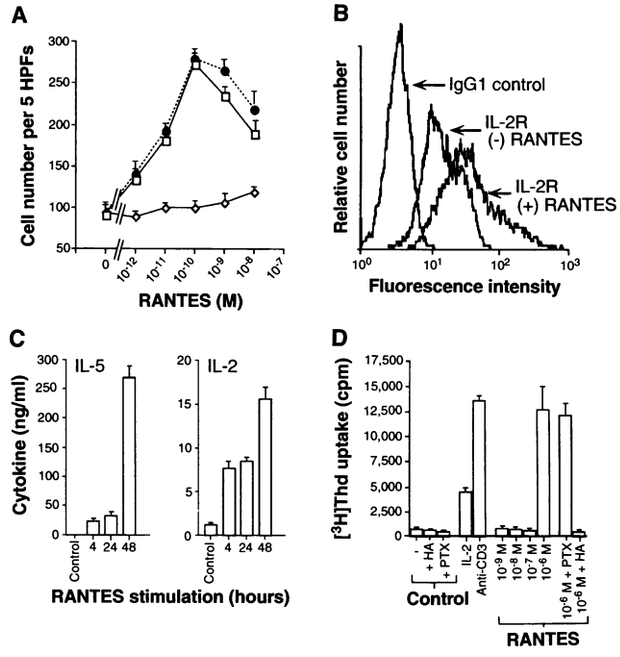

Fig. 4. Functional assays of T cell chemotaxis and activation. (**A**) Chemotaxis of T cells induced by RANTES (●) was inhibited by PTX (◇) and unaffected by HA (□). Cells were incubated with PTX (100 ng/ml, 18 hours) or HA (2 μM, 18 hours), washed (250*g*, 10 min), resuspended in normal cell culture medium, and assayed as previously described (*21*). Each point represents the mean ± SEM number of cells per five high-power fields (HPFs) for four experiments performed in duplicate. (**B**) Effect of RANTES (1 μM) on surface expression of the IL-2 receptor (IL-2R). Cells were cultured in serum- and IL-2–free medium and then stimulated with RANTES for 48 hours. IL-2R expression was measured by fluorescence-activated cell sorting (*22*) with a specific antibody to IL-2R. (**C**) Effect of RANTES on cytokine production. Quiescent T cells for serum and IL-2, were incubated for 4, 24, or 48 hours with 1 μM RANTES, after which the supernatants were collected and assayed for IL-2 or IL-5 by specific enzyme-linked immunosorbent assays (*23*). Values are means ± SEM of three experiments. (**D**) The effect of RANTES on T cell proliferation. Quiescent cells were incubated with no treatment (−), HA (2 μM), PTX (100 ng/ml), anti-CD3 (5 μg/ml), or the indicated concentrations of RANTES for 48 hours. Each histogram represents the mean ± SEM of [^{3}H]thymidine (Thd) incorporation (counts per minute) for five experiments. The bar representing IL-2 alone demonstrates the normal, basal proliferation (survival) level of the clone under typical culture conditions.

and PTK pathways were assessed with the use of several assays. RANTES-induced chemotaxis was completely inhibited after incubation of T cells with PTX, but was unaffected by HA (Fig. 4A). T cell activation, characterized by the up-regulation of the IL-2 receptor and the production of cytokines, was also affected by RANTES, which consistently increased IL-2 receptor expression (Fig. 4B) and markedly increased both IL-2 and IL-5 production (Fig. 4C). RANTES had no measurable effect on IL-4 or interferon γ. Lastly, T cell proliferation was markedly increased by RANTES. At a concentration (1 μM) that triggered the second phase of Ca^{2+} mobilization, RANTES induced a >10-fold increase in T cell proliferation, similar to the effect of anti-CD3 (Fig. 4D). RANTES-induced proliferation was completely abolished by treatment with HA, but was unaffected by PTX. The chemokines MCP-1 and MIP-1α, at the same concentration as RANTES, failed to elicit similar responses. Thus, RANTES, in isolation of other activating or costimulating agents, can functionally induce T cell proliferation in a manner similar to mitogenic stimulation.

The RANTES-induced responses observed in our study may not be mediated exclusively through the C-C CKR-1. We have isolated another 7TM receptor, showing substantial homology to C-C CKR-1, from the T cell clone used here (*18*). It is unlikely that any of the antigen-independent activation signals occur via stimulation of the TCR at high concentrations of RANTES. Related chemokines with similar charge profiles and aggregation properties induced neither the second phase of the signaling response nor T cell proliferation when used at equimolar concentrations. Moreover, several Jurkat T cell lines responded to TCR stimulation with anti-CD3 but not to RANTES, even at concentrations up to several micromolar. Indeed, the bioactive concentration of RANTES in the present study is still an open issue. Most chemokines are thought to be active in either the monomer or dimer (unaggregated) form (*19*). Because RANTES is almost completely aggregated in solution at a pH of >4.0 (*19*), it is likely that the actual effective concentrations of RANTES used in this study are less than those listed. Additionally, physiological concentrations of chemokines in the micromolar range have been posited. Chemokines show high affinities for cell surface proteoglycans (*20*), as a result of which they are sequestered and presented to target cells at high concentrations within a local microenvironment.

RANTES-induced signaling in T cells appears distinct from that described for ligands of other 7TM receptors in that PTKs are recruited together with G proteins. The demonstration of elaborate parallel molecular signals induced by RANTES suggests a complex physiological mechanism for control of multiple T cell functions. A coordinated program can be envisaged whereby G protein–mediated migration at low relative concentrations of chemokine leads to infiltration at sites of high concentrations of RANTES sequestered by proteoglycans, resulting in activation and proliferation by means of the PTK cascade. This scenario may have implications for chronic inflammatory pathologies for which the identification of persistent antigen has been elusive.

REFERENCES AND NOTES

1. T. J. Schall, K. Bacon, K. J. Toy, D. V. Goeddel, *Nature* **347**, 669 (1990); T. J. Schall, in *The Cytokine Handbook*, A. Thompson, Ed. (Academic Press, New York, ed. 2, 1994), pp. 419–460; K. Neote, D. DiGregorio, J. Y. Mak, R. Horuk, T. J. Schall, *Cell* **72**, 415 (1993).
2. S. C. Bischoff *et al.*, *Eur. J. Immunol.* **23**, 761 (1993); G. Van Riper *et al.*, *J. Exp. Med.* **177**, 851 (1993); S. Sozzani *et al.*, *J. Immunol.* **152**, 3615 (1994).
3. K. B. Bacon and R. D. R. Camp, *Biochem. Biophys. Res. Commun.* **169**, 1099 (1990); K. B. Bacon, D. G. Quinn, J.-P. Aubry, R. D. R. Camp, *Blood* **81**, 430 (1993); K. B. Bacon *et al.*, *J. Immunol.* **154**, 3654 (1995).
4. B. A. Premack and P. Gardner, *Am. J. Physiol.* **263**, C1115 (1992); G. R. Crabtree and N. A. Clipstone, *Annu. Rev. Biochem.* **63**, 1045 (1994); A. Weiss, *Cell* **73**, 209 (1993); T. Mustelin, *Immunity* **1**, 351 (1994); A. C. Chan, D. M. Desai, A. Weiss, *Annu. Rev. Immunol.* **12**, 555 (1994).
5. L. S. Gray, K. S. Huber, M. C. Gray, E. L. Hewett, V. H. Engelhard, *J. Immunol.* **142**, 1631 (1989); J. Modesto, J. P. Breittmayer, N. Grenier-Brossette, M. Fehlmann, J. L. Cousin, *Cell Signal.* **3**, 25 (1991).
6. T. Mustelin, K. M. Coggeshall, N. Isakov, A. Altman, *Science* **247**, 1584 (1990); C. H. June, M. C. Fletcher, J. A. Ledbetter, L. E. Samelson, *J. Immunol.* **144**, 1591 (1990).
7. M.-G. Roncarolo *et al.*, *J. Exp. Med.* **168**, 2139 (1989). A tetanus toxoid–specific normal human T cell clone was stimulated with irradiated human peripheral blood mononuclear cells and the Epstein-Barr virus–transformed B cell line JY in complete medium [Iscove's modified Dulbecco's medium containing 10% heat-inactivated fetal bovine serum, 25 mM Hepes (pH 7.4), 2 mM L-glutamine, and gentamycin (50 μg/ml)] containing phytohemagglutinin (10 μg/ml) (HA-16; Burroughs Wellcome). After 4 to 5 days, the proliferating cells were incubated with complete medium containing human recombinant interleukin-2 (IL-2) (20 U/ml) (DNAX Research Institute) and the medium was changed every 14 to 18 days. The clone was of the T helper cell 0 (T_H0) type, expressing TCRαβ and CD4 and producing the cytokines IL-3, granulocyte-macrophage colony-stimulating factor, IL-4, IL-5, IL-2, and interferon γ.
8. Cloned human T cells were loaded with 2 μM indo-1 acetoxymethyl ester in complete growth medium at 20°C for 45 min. Cells were then washed, resuspended in Hanks' balanced salt solution (HBSS) [2 mM $CaCl_2$, 145 mM NaCl, 5 mM KCl, 1 mM $MgCl_2$, 5 mM D-glucose, 20 mM Hepes (pH 7.3)] containing 1% bovine serum albumin (BSA), and maintained at 20°C for up to 2 hours. RANTES (R&D Systems) was added to ~5×10^5 cells suspended in 2 ml of HBSS and maintained at 37°C in a constantly stirred acrylic cuvette. Fluorescence measurements to determine $[Ca^{2+}]_i$ were performed with a Photon Technologies spectrofluorometer at an excitation wavelength of 350 nm (4-nm bandwidth) and with dual simultaneous monitoring of emission at 405 and 485 nm (10-nm bandwidth). The ratio of emission at 405/485 nm was measured at a rate of 2 Hz. Final $[Ca^{2+}]_i$ values were calculated from the ratio according to the standard equation with a dissociation constant of 250 nM for indo-1 [G. Grynkiewicz, M. Poenie, R. Y. Tsien, *J. Biol. Chem.* **260**, 3440 (1985)] and applying a viscosity correction factor of 0.85 for indo-1 in cytosol [M. Poenie, *Cell Calcium* **11**, 85 (1990)].
9. The RANTES-induced responses presented here are not specific to the T cell clone used in this study. In the Ca^{2+}-response experiments, as in the subsequent measurements of tyrosine phosphorylation, cytokine production, and cellular proliferation, we obtained similar results with freshly isolated human peripheral blood T lymphocytes as well as several other human T cell and natural killer cell clones. In peripheral blood lymphocytes the calcium responses have qualitatively similar biphasic kinetics, but of lesser magnitudes, perhaps suggesting subpopulation of responding cells.
10. Conventional whole-cell patch-clamp recordings [O. P. Hamill, A. Marty, E. Neher, B. Sakmann, F. J. Sigworth, *Pfluegers Arch.* **391**, 85 (1981)] were performed with a List EPC-7 patch-clamp amplifier, with the current output filtered at 1.5 kHz with an external eight-pole Bessel filter. During voltage-clamp experiments, the membrane currents were digitized at 12-bit resolution with an Axon Instruments TL-1 interface and pClamp 6.0 analysis software. The pipette solution contained 120 mM cesium aspartate, 10 mM CsCl, 2 mM $MgCl_2$, 0.5 mM adenosine triphosphate (Mg^{2+} salt), 2 mM $CaCl_2$, 10 mM Cs_4BAPTA, and 10 mM Hepes (pH 7.3). The substitution of aspartate for Cl^- gives a calculated Cl^- reversal potential of −60 mV when used with the extracellular solution described below. Na^+- and K^+-free extracellular solutions containing *N*-methyl-D-glutamate ($NMDG^+$) as the main cation [160 mM $NMDG^+$ Cl^-, 2 mM $CaCl_2$, 1 mM $MgCl_2$, 5 mM D-glucose, 10 mM Hepes (pH 7.3)] were used to minimize currents flowing through voltage-gated Na^+ or K^+ channels. For external test solutions containing >2 mM Ca^{2+}, the test ion was substituted for $NMDG^+$. During patch-clamp experiments, T cells were maintained at 30°C on the temperature-controlled stage of a Nikon Diaphot microscope. The cells were plated onto a #1 cover glass that formed the bottom of a 0.2-ml acrylic plastic perfusion chamber. Prewarmed solutions were changed by a rapid gravity-fed perfusion system that exchanged the entire bath with a time constant of ~1 s. We collected data generated by both voltage steps and voltage ramps during an experiment. After RANTES addition, the membrane currents changed rapidly, making it difficult to complete a standard voltage-step protocol. We therefore followed the rapid changes in membrane current with 320-ms voltage ramps from −100 to +60 mV (depolarization rate of 0.5 mV/ms) and a holding potential of −60 mV. The holding current in Fig. 1D was digitized at a frequency of 1 Hz. The ramp currents in Fig. 1E were digitized at a frequency of 2 kHz and digitally filtered at 300 Hz. The *I-V* curves show the membrane voltage as approximated from the command voltage and have not been corrected for a +5- to +7-mV tip potential that is present in these solutions.
11. K. B. Bacon, B. A. Premack, P. Gardner, T. J. Schall, data not shown.
12. M. Hoth and R. Penner, *Nature* **355**, 353 (1992).
13. T. V. McDonald, B. A. Premack, P. Gardner, *J. Biol. Chem.* **268**, 3889 (1993); A. Zweifach and R. S. Lewis, *Proc. Natl. Acad. Sci. U.S.A.* **90**, 6295 (1993); B. A. Premack, T. V. McDonald, P. Gardner, *J. Immunol.* **152**, 5226 (1994); B. A. Premack and P. Gardner, *Adv. Exp. Med. Biol.* **365**, 91 (1994).
14. T. J. Schall and K. B. Bacon, *Curr. Opin. Immunol.* **6**, 865 (1994).
15. Chemokine-induced Ca^{2+} mobilization was shown to be inhibited by PTX in human embryonic kidney (HEK) 293 cells stably transfected with the human C-C CKR-1 receptor.
16. The PTK inhibitors genistein and HA (Calbiochem) were chosen because of their membrane permeability. HA was the most potent inhibitor (50% inhibition at 0.2 μM); genistein also exhibited partial (~50%) inhibition of PTK activation (at 10 μM), but was not used in any of the present experiments because it is a less selective inhibitor of tyrosine kinases than HA.

All inhibitors were tested from 0.1 to 10 μM and viability was monitored by trypan blue exclusion. The final concentrations of HA used to inhibit tyrosine kinases in this study were approximately 1/10 to 1/20 of that required for direct inhibition of Ca^{2+} entry into T cells.

17. Cells were incubated for 48 hours in IL-2–free culture medium containing 0.5% serum. Cell viability was >95%. Inhibitor-pretreated or untreated lymphocytes were then stimulated with RANTES for 30 s to 5 min, rapidly separated by centrifugation at 4°C, and lysed for 15 min on ice with periodic mixing in lysis buffer [1% Triton X-100, 20 mM tris-HCl (pH 8.0), 137 mM NaCl, 15% glycerol, 5 mM EDTA] containing phosphatase and protease inhibitors [1 mM phenylmethylsulfonyl fluoride, aprotinin (10 μg/ml), leupeptin (10 μg/ml), 1 mM sodium orthovanadate, 1 mM EGTA, 100 μM β-glycerophosphate]. The lysates were analyzed under reducing conditions on 10% SDS-polyacrylamide gels (Novex). Resolved proteins were transferred to activated Immobilon P membranes (Millipore) for immunoblot analysis. Membranes were incubated first in tris-buffered saline (TBS) containing 5% BSA, 0.1% Tween-20, and 0.05% thimerosol and then overnight with antibodies (4G10) to phosphotyrosine (1 μg/ml) (UBI). The filters were then washed extensively (TBS containing 0.5% NP-40), incubated with secondary horseradish peroxidase–coupled antibodies to mouse immunoglobulin (Amersham), washed again, incubated with ECL reagent (Amersham), and exposed to BIOMAX-MR film (Eastman Kodak).
18. Cloning studies, with primers targeted to homologous domains of the chemokine 7TM receptor family, have identified a potentially uncharacterized receptor in the T cell clone and peripheral blood lymphocytes.
19. N. J. Skelton, F. Aspiras, T. Schall, *Biochemistry* **34**, 5329 (1995); K. Rajarathnum *et al.*, *Science* **264**, 90 (1994); G. J. Graham *et al.*, *J. Biol. Chem.* **269**, 4974 (1994).
20. L. M. C. Webb, M. U. Ehrengruber, I. Clark-Lewis, M. Baggiolini, A. Rot, *Proc. Natl. Acad. Sci. U.S.A.* **90**, 7158 (1993); D. P. Witt and A. D. Lander, *Curr. Biol.* **4**, 394 (1994); Y. Tanaka *et al.*, *Nature* **361**, 79 (1993).
21. K. B. Bacon, R. D. Camp, F. M. Cunningham, P. M. Woollard, *Br. J. Pharmacol.* **95**, 966 (1988).
22. Fluorescence-activated cell sorting (FACS) was performed according to standard methods. Quiescent lymphocytes were left unstimulated or were stimulated for 48 hours with RANTES (1 μM), washed in phosphate-buffered saline containing 0.05% NaN_3 and 1% BSA, incubated at a concentration of 2×10^5 cells per well in a 96-well conical plate (Costar Serocluster) with fluorescein isothiocyanate–coupled antibodies to human CD25 (IL-2R) (Becton Dickinson) for 30 min, washed three times, and then analyzed with a Becton Dickinson FACScan. It was necessary to render the cells quiescent before FACS analysis because the cells are maintained in IL-2–containing medium; thus, the level of IL-2 receptor expression is high and small changes are masked.
23. Enzyme-linked immunosorbent assay measurements were made according to standard protocols with quiescent T cells, in order to avoid the high basal expression of cytokines such as IL-2, IL-5, and IL-4. Antibodies [anti–IL-5 (39D10), rat immunoglobulin (Ig) G2a; anti–IL-4 (8D4-8), mouse IgG1; anti–interferon γ (A35), mouse IgG1; anti–IL-2 (BG-5), mouse IgG1] (DNAX) were coated onto the wells of a 96-well polyvinyl chloride plate and incubated for 2 hours at 37°C. After washing the wells, the samples were incubated with the coating antibody for 2 hours at room temperature, after which the wells were washed and incubated for 1 hour at room temperature with nitroiodophenylacetate-coupled secondary antibodies (50 μg/ml) [anti–IL-5 (5A10), rat IgG2a; anti–IL-4 (MP4-25D2), rat IgG1; anti–interferon γ (B27), mouse IgG1; anti–IL-2, goat polyclonal] (DNAX). Immune complexes were revealed by incubation with tertiary horseradish peroxidase–coupled antibodies to nitroiodophenylacetate for 1 hour at room temperature. After incubation, ABTS solution was added and absorbance at 405 to 600 nm measured after the color had developed. Results were analyzed with SoftMax software (Molecular Devices) to obtain absolute protein values.
24. We thank H. Yssel (DNAX) for the initial provision of the T cell clone. B.A.P. was supported by NIH fellowship GM07065. B.A.P. and P.G. were also supported by American Cancer Society grant DB-26E. DNAX Research Institute is supported by Schering Plough.

27 April 1995; accepted 18 July 1995

Regulation of Hippocampal Transmitter Release During Development and Long-Term Potentiation

Vadim Y. Bolshakov and Steven A. Siegelbaum

Developmental changes in rat hippocampal transmitter release and synaptic plasticity were investigated. Recordings from pairs of pyramidal neurons in slices showed that an action potential in a CA3 neuron released only a single quantum of transmitter onto a CA1 neuron. Failures of synaptic transmission reflected probabilistic transmitter release. The probability of release (P_r) was 0.9 in 4- to 8-day-old rats and decreased to less than 0.5 at 2 to 3 weeks. Long-term potentiation (LTP) in 2- to 3-week-old rats was associated with an increase in P_r from a single synaptic site. The high initial P_r in 4- to 8-day-old rats normally occludes the expression of LTP at this stage.

Long-term potentiation (LTP) (*1*) and long-term depression (LTD) (*2*) of hippocampal synaptic transmission are opposing forms of activity-dependent plasticity that may underlie learning and memory and the fine tuning of synaptic connections during development (*3*). The expression of hippocampal LTP and LTD in rats changes markedly during the first 3 weeks after birth, a critical period in the establishment of synaptic connections (*4*). Whereas LTP is observed only in rats that are >2 weeks old (*5*, *6*), LTD is most prominent during the first 10 days after birth (*6*, *7*). This complementary pattern of expression of LTP and LTD is likely important for the formation of the normal pattern of synaptic connections and early learning and memory. However, controversy surrounds the basic properties of synaptic transmission and long-term plasticity in the hippocampus (*1*, *8*), and the mechanisms underlying these developmental changes remain unknown. This uncertainty is attributable, in part, to difficulties in recording from individual pairs of synaptically connected hippocampal neurons; most studies have relied on recordings from populations of pre- and postsynaptic cells (*1*, *8*).

We have now used two approaches that permit the routine recording of synaptic transmission between single CA3 and CA1 pyramidal neurons in hippocampal slices: (i) dual whole-cell patch clamp recording (Fig. 1A) (*9*, *10*); and (ii) focal stimulation of a single presynaptic neuron, by pressing an extracellular stimulating patch pipette onto an individual CA3 cell body (*11*, *12*), and whole-cell recording from a postsynaptic CA1 neuron. Both methods resulted in identical postsynaptic responses (*13*). However, most experiments (24 of 36) were performed with extracellular stimulation because of the difficulty in obtaining stable dual whole-cell recordings.

A given CA1 neuron received functional synaptic input from ~5% of the CA3 neurons tested (Fig. 1A) (*14*). In a synaptically connected pair of neurons from a 6-day-old rat, most CA3 action potentials elicited an excitatory postsynaptic current (EPSC) of ~ −4 pA in a CA1 cell (Fig. 1B). Some stimuli failed to elicit an EPSC. A frequency histogram of EPSC amplitudes showed two prominent peaks that were fitted by the sum of two Gaussian functions (Fig. 1C). One peak, centered at 0 pA with a standard deviation identical to that of the background noise, reflected failures of transmission. The second peak, centered at ~−4 pA, contained most events and reflected successes of transmission. There were no additional peaks at higher current levels. In synapses from young animals (4 to 8 days old), the fraction of successes was consistently high and averaged 0.9 (*13*). In comparison, in slices from older rats (13 to 23 days old), the fraction of successes was significantly lower (<0.5) (Fig. 1, D to F) in agreement with previous, less direct results (*15*). In other respects, however, transmission in older rats resembled that in younger rats: The EPSC amplitude histogram showed only two peaks, one at 0 pA and one at ~−4 pA (Fig. 1, D and E).

The simplest interpretation of these results, based on the classical quantal theory of Katz (*16*), is that a given CA3 neuron makes only a single synaptic contact with a given CA1 neuron. At this contact, a presynaptic action potential either fails to release transmitter or evokes an EPSC that

Center for Neurobiology and Behavior, Department of Pharmacology, and Howard Hughes Medical Institute, College of Physicians and Surgeons, Columbia University, 722 West 168th Street, New York, NY 10032, USA.